

# Modeling of gamma-radiation impact on transmission characteristics of optical glasses

A.I. Gusarov<sup>\*a</sup>, D.B. Doyle<sup>\*\*b</sup>

<sup>a</sup>Mulitel asbl; <sup>b</sup>European Space Research Technology Centre

## ABSTRACT

Optical systems operating in space must maintain their performance over long mission times. Glasses are well known to darken upon exposure to radiation, due to formation of color centers, resulting in performance degradation. Despite increasing demand, an approach which would allow accurate prediction of the end-of-life performance characteristics of space optical instruments, has not been elaborated yet. We propose here a phenomenological methodology that should help to solve the problem. In our model, functional dependencies describing defect generation and annealing are derived from mathematical models, taking into account dose levels and irradiation times relevant for space missions. Numerical values for the parameters come from experimental data. Our experimental methodology is also described. We apply this model to analyze the results obtained for BK7 glass subject to Co<sup>60</sup> gamma-radiation.

## 1. INTRODUCTION

Optical systems operating in space must maintain their performance over long mission times. Among other factors, the impact of radiation on optical instrumentation has remained a major concern since the beginning of space optics. Glasses are well known to darken upon exposure to radiation, due to formation of color centers, resulting in performance degradation caused by the power budget limitation. We propose here a phenomenological approach that allows end of life spectral transmission performance characteristics to be predicted for space optical systems.

## 2. COLOR CENTER MODEL

Significant progress in the understanding of radiation effects in optical materials has been achieved during the last few decades. Transmission degradation under radiation is a consequence of the generation of radiation defects, which absorb light. Such defects correspond to electronic states, which are not present in the glass before irradiation. Optical transitions related with those states give rise to an additional absorption in the visible. A decrease of the density of initial electronic states corresponds to a decrease of absorption in the region of initial absorption bands. However, such induced transparency is usually not of interest because, before exposure to radiation, glasses are transparent in the working spectral range.

In general, an electronic state can be converted to another one by radiation. The most sensitive to radiation are dangling bonds, oxygen bridges, over-coordinated atoms, i.e. deviations from the "ideal" random network. The concentration of such radiation precursors is usually much lower than the concentration of normal bonds.

Radiation defects in glass are not stable. They can be thermally-, optically- or radiation-transformed to other configurations. The concentration of radiation defects changes after the end of irradiation, some of them can be completely annealed, but most defects are meta-stable and are characterized by very long relaxation times.

The first order evolution kinetics of the precursors concentration is described by a differential equation, which takes into account both generation and annealing:

$$\frac{dn}{dt} = -k_g n + k_a (n_0 - n) \quad (2.1)$$

---

\* e-mail: gusarov@telecom.fpms.ac.be; bd. Dolez 31, B-7000 Mons, Belgium; \*\* e-mail: Dominic.Doyle@esa.int, European Space Agency, European Space Research Technology Centre, 2200 AG Noordwijk, The Netherlands

where  $n_0$  and  $n(t)$  are the initial and instantaneous concentrations of precursors, and where  $k_g$  and  $k_a$  are the rates of generation and annealing of the defects, respectively. The first term describes the decrease of concentration due to transformation of precursors to metastable defects and the second one takes into account the defect annealing. The rate of defect generation is proportional to the radiation dose rate  $R$ :

$$k_g = cR \quad (2.2)$$

where the constant  $c$  depends on material characteristics only, provided that interaction of the excited states is not important. It can be analytically computed based on known models of defect generation. However such computations are rather complicated and the accuracy is not very high. It seems more realistic to find  $c$  using experimental data. Solving (2.1) for the defect concentration  $n_i$ , gives:

$$n_i(k_a) = n_0 \frac{k_g}{k_a + k_g} \left[ 1 - \exp\left(-[k_a + k_g]t\right) \right]. \quad (2.3)$$

The index “ $i$ ” is added in order to distinguish different types of defects. This solution shows that at the initial stage the defect concentration grows linearly, and it saturates with increase of irradiation time. The saturation level depends on both the generation and the annealing rates. If relaxation is very fast ( $k_g \ll k_a$ ) the saturation level is significantly smaller than the level defined by the precursor concentration. In the absence of relaxation ( $k_a = 0$ ) we can rewrite Eq.(2.3) as

$$n_i = n_{0i} \left[ 1 - \exp(-cD) \right]. \quad (2.4)$$

where  $D$  is the accumulated dose, which makes it evident that  $c$  is the inverse of the saturating radiation dose  $D_s$ . In disordered materials relaxation is characterized by a broad distribution of the relaxation rates  $\varphi(k)$ :

$$n_i = \int dk_a \varphi(k_a) n_i(k_a) \quad (2.5)$$

This distribution is temperature dependent with parameters different for each defect type.

The amorphous nature of glass results also in inhomogeneous broadening of defect-related optical transitions, which are well characterized as Gaussian bands. The induced absorption coefficient  $\Delta a_i$  is proportional to the defect concentration. Therefore

$$\Delta a_i(\omega) = A_i \exp(-(\omega - \omega_{0i})^2 / 2\sigma_i^2); \quad A_i = s_i n_i \quad (2.6)$$

where  $\omega_{0i}$  is the central frequency,  $\sigma_i$  is the band width and  $s_i$  defines the amplitude of the absorption band.

For low doses  $n_i(k_a) \approx n_0 cD$  and

$$A_i \approx \alpha_{Di} D, \quad \alpha_{Di} = c s_i n_{0i} = s_i n_{0i} / D_{si}, \quad (2.7)$$

i.e.  $\alpha_{Di}$  is the dose coefficient (DC) for the absorption band “ $i$ ”. Using this DC we can represent  $A_i$  as

$$A_i(k_a) = \alpha_{Di} Z^{-1} \left[ 1 - \exp(-ZD) \right]; \quad Z = k_a / R + \alpha_{Di} / a_{0i}; \quad a_{0i} = s_i n_{0i}. \quad (2.8)$$

which is reduced to the previous expression for low doses ( $\alpha_{Di} D \ll a_{0i}$ ) and slow relaxation ( $k_a t \ll 1$ ). For a given relaxation kinetics, defect accumulation is characterized by the DC  $\alpha_{Di}$  and the parameter  $a_{0i}$ . This latter parameter has the meaning of the maximal achievable absorption in the case of a fast irradiation.

Finally, it is necessary to take into account that the absorption spectrum is composed of a number of absorption bands

$$\Delta a(\omega) = \sum_{i=1}^N A_i \exp(-(\omega - \omega_{0i})^2 / 2\sigma_i^2). \quad (2.9)$$

We have now obtained a set of formulae which allow the induced absorption under radiation or after the end of irradiation to be described. The practical application of this approach requires the kinetic parameters defining defect generation ( $\alpha_{Di}$  and  $a_{0i}$ ), annealing ( $\varphi_i$ ), along with spectroscopic parameters ( $\omega_{0i}$ ,  $\sigma_i$ ) to be known for each type of defect. In the next section we show how these parameters can be found from the optical transmission measurements.

### 3. EXPERIMENTAL PROCEDURE

We have selected BK7 (Schott) glass for the present study. The samples were polished discs 0.2mm and 5mm thick. The optical transmission spectra were recorded in the spectral range from 200 to 800 nm using a commercial double-beam spectro-photometer. The natural logarithm of the ratio of the transmission before irradiation to that after irradiation, normalized by the sample thickness, gives the radiation-induced absorption coefficient.

A Co<sup>60</sup> source with a dose-rate of 6 krad/h (water) at the samples location was used for  $\gamma$ -irradiation of the samples (1 rad corresponds to  $10^{-2}$  Joules of energy absorbed by 1 kg of material, the SI unit of absorbed dose is the Gray = 100 rads). Irradiation was performed in a stepwise dose-accumulation manner. First the samples were irradiated with a dose of 400 krad. Optical measurements were performed with a 2-hours delay. Then the samples were irradiated again, so that the total accumulated dose reached 800 krad. After the end of irradiation transmission spectra were measured several times in a time interval up to 65 days in order to monitor post-radiation relaxation.

#### 4. EXPERIMENTAL DATA ANALYSIS

Several induced attenuation spectra of a particular sample of BK7 glass are shown in Figure 1. In order to construct the kinetic curves it is necessary to resolve the absorption spectra into individual absorption bands. As a result of non-orthogonality of the Gaussians such decompositions are not unique and additional information is required to obtain a physically meaningful result. Based on the data available in the literature we assume that for relevant radiation loads the experimental spectra in the range 230-800 nm can be described with four bands. We assumed also that the central energy and the width of those bands are not changed either during the experiment or after the end of irradiation. It is necessary to note that the selection of the number of the bands is a very important point and it can not be done automatically. Moreover, a good fit does not guarantee that the selected bands are physically meaningful. The condition required is that physical functions must be used in order to be able to analyze the relaxation kinetics. The parameters of the bands are given in Table. 1. The values were found by averaging the values obtained in an independent fit of each induced attenuation spectrum.

Band	1	2	3	4
Center, eV	2.03	2.88	4.26	5.35
Width, eV	0.21	0.58	0.65	0.32

Table. 1 Parameters of the absorption bands used to approximate the induced absorption spectra.

Using these values and allowing only the amplitudes of the bands to vary we have obtained a good fit of the all experimentally induced absorption spectra (e.g. Figure 1, Figure 2 and Figure 3). The results are summarized in Figure 4. For the low-energy bands (1 to 3) the amplitude decreases monotonously after the end of irradiation. At present we can not draw definite conclusion about the UV 5.35-eV band. Its amplitude shows irregular behavior, which is probably a consequence of a lack of accuracy in short-wavelength measurements (Figure 6). The primary concern of the present study is transmission behavior in the visible. The 5.35-eV band gives no contribution for wavelengths longer than 300 nm (4.1 eV). Therefore, the first 3-bands are sufficient to describe the induced absorption in the visible. However, accounting of the UV-band is required to define the amplitudes correctly.

The kinetic curves contain the required information about both the defect accumulation and the annealing. Relaxation in strongly-correlated systems is usually non-exponential. It can be seen that the Debye-type (exponential) kinetics

$$q(t) = \exp(-t/\tau), \quad (4.1)$$

where  $\tau$  is the Debye relaxation time, are not sufficient to achieve a good description of the experimental results (Figure 4). A simple approach used in such situations is the introduction of a multi-exponential relaxation

$$q(t) = \sum_{i=1}^N a_i \exp(-t/\tau_i), \quad N > 4, \quad (4.2)$$

which means that  $2N-1 > 7$  parameters are used to describe experimental data. The application of this approach in our case is not feasible due to the limited set of experimental data. Therefore, it is of interest to test the stretched-exponent (Kohlrausch) law, which is known to give very good results:

$$q(t) = \exp(-(t/\tau_0)^\alpha), \quad 0 < \alpha < 1, \quad (4.3)$$

where  $\tau_0$  is the characteristic relaxation time and  $\alpha$  is the index of the fractional-exponential function. This function gives a good description of the experimental data for 3 to 71 days of the experiment (Figure 5). The parameters  $\{\tau_0, \alpha\}$  are given in Table. 2. Deviations can be expected for shorter and longer times.

Band center, eV	2.03	2.88	4.26
$\tau_0$ , days	200.9	758.5	8847
$\alpha$	0.723	0.360	0.275

Table. 2 Parameters of the Kohlrausch function for the three visible absorption bands in BK7.

If we consider the non-exponential relaxation to be a superposition of the contributions made by elementary exponential relaxation processes

$$q(t) = \int_0^{\infty} dk \exp(-kt) \varphi(k), \quad (4.4)$$

then the distribution of the relaxation rates is given by the inverse of the Laplace transformation

$$\varphi(k) = \tau_0 \int_0^{\infty} \frac{dz}{\pi} \cos \left[ k \tau_0 z - z^{\alpha} \sin\left(\alpha \frac{\pi}{2}\right) \right] \exp \left[ -z^{\alpha} \sin\left(\alpha \frac{\pi}{2}\right) \right]. \quad (4.5)$$

An example of the relaxation rates distribution is given in Figure 7 for the 2.03 eV band.

Once  $\varphi(k)$  is known, it is possible to find from the accumulation part of the kinetic curves the dose coefficients and the saturated absorption for each type of defect via solution of a minimization problem for a system of integral equations. The problem is greatly simplified in the case of a high dose-rate irradiation, when the effect of relaxation during irradiation can be neglected.

We have found the following values from our experimental data

Band center, eV	2.03	2.88	4.26
$\alpha_{Di}$ , (cm·krad) <sup>-1</sup>	0.266·10 <sup>-2</sup>	1.14·10 <sup>-2</sup>	2.45·10 <sup>-2</sup>
$a_{0i}$ , cm <sup>-1</sup>	1.22	6.79	16.5

Table. 3 Dose coefficients and saturated absorption coefficients.

These results show that the concentration-related saturation starts to play a role for radiation doses above 500 krad. For the relatively low radiation loads typical of most space applications, saturation is not significant and the defect accumulation kinetics can be characterized with only the dose coefficient (for each absorption band). This is a reasonable estimation, although the accuracy of the data in Table. 3 is not very high, because we have only two accumulation measurements.

We have now all the parameters required for computation of the internal transmission evolution under  $\gamma$ -radiation. The results of computations for a 5-cm thick BK7 glass plate  $\gamma$ -irradiated over 1 year with the total accumulated dose of 100 krad are given in Figure 8. The simulation was made for four wavelengths,  $\lambda_r = 706$ ,  $\lambda_C = 656$ ,  $\lambda_D = 589$  and  $\lambda_F = 486$  nm. The transmission degradation is more significant for shorter wavelengths as expected.

## 5. CONCLUSIONS

A model that allows computation of the transmission degradation of glass in a (space) radiation environment was developed. The approach is based on the color center model and is universally applicable in the sense that it allows description of the effect of radiation in any glass under any radiation regime. The required spectroscopic, accumulation, and relaxation parameters of the absorption bands can be found by following the described experimental procedure.

The application of the methodology was demonstrated using results of transmission measurements on BK7 glass irradiated using a Co<sup>60</sup> source. The results emphasize the importance of optical measurements in a wide spectral interval and for long relaxation times. The total accumulated dose must correspond to the expected radiation loads for a particular instrument scenario. The dose-rate dependence is taken into account by the model. While the near-Earth space radiation environment is dominated by protons and electrons, we believe that the kinetic data and the saturating doses are independent of the type of ionizing radiation and only the values of the dose coefficients are radiation-specific.

The present model has several limitations. It considers isothermal irradiation and annealing. To extend it to non-isothermal conditions, the temperature dependence of the relaxation constants is required to be taken into account.

We have found that the stretched-exponent gives a good description of the experimental data for the intermediate time-scale (3 – 70 days). It may be expected that the kinetics is different for shorter or longer times. Shorter time scales are in any case not of interest for space applications, but time-scales of years still requires proper consideration.

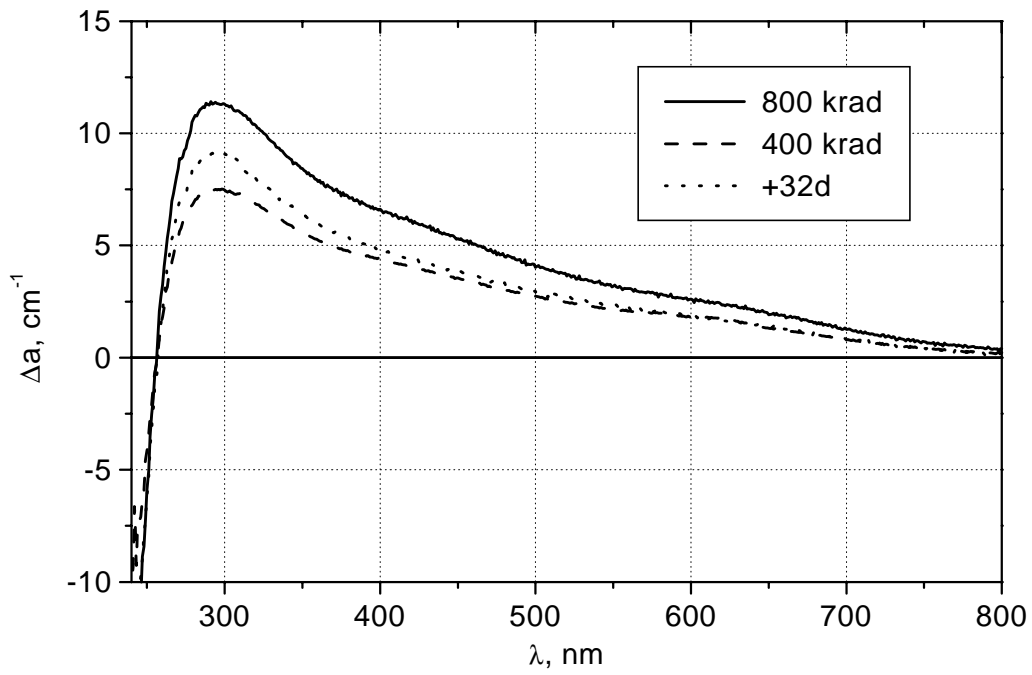


Figure 1 Spectra of induced attenuation measured after two consecutive irradiations and also 32 days after the end of the second irradiation.

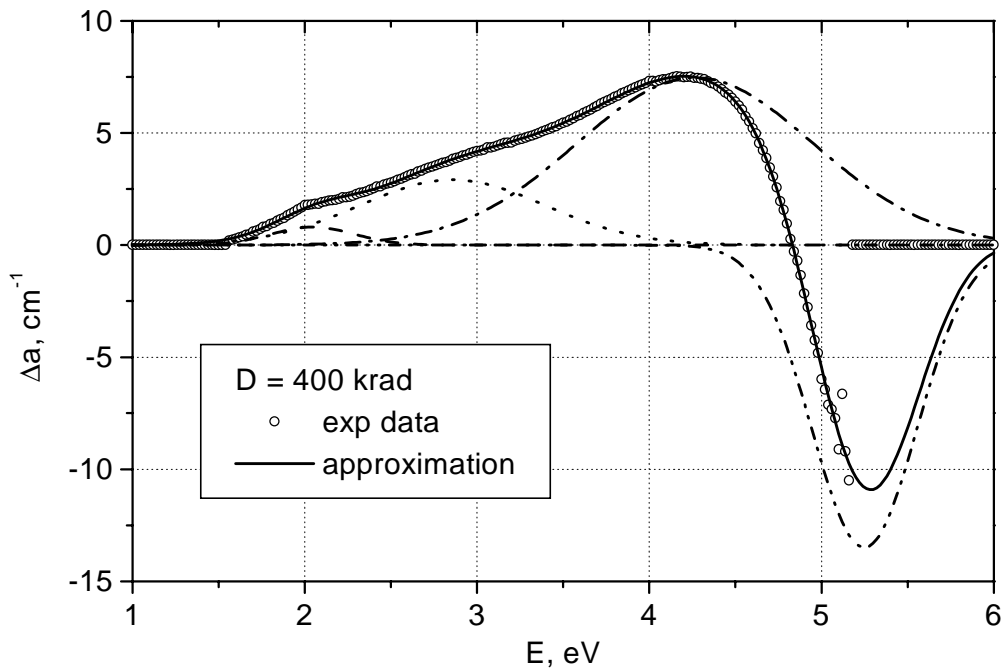


Figure 2 Decomposition of the induced attenuation spectrum into 4 bands after the first dose  $D = 400$  krad.

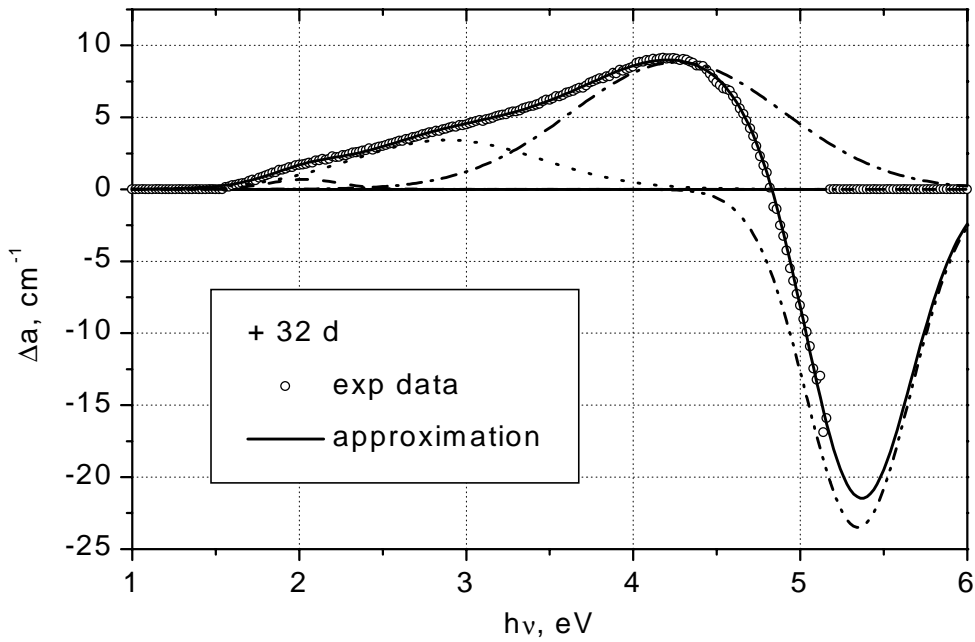


Figure 3 Decomposition of the induced attenuation spectrum into 4 bands. D = 800 krad, 32 days after the end of irradiation.

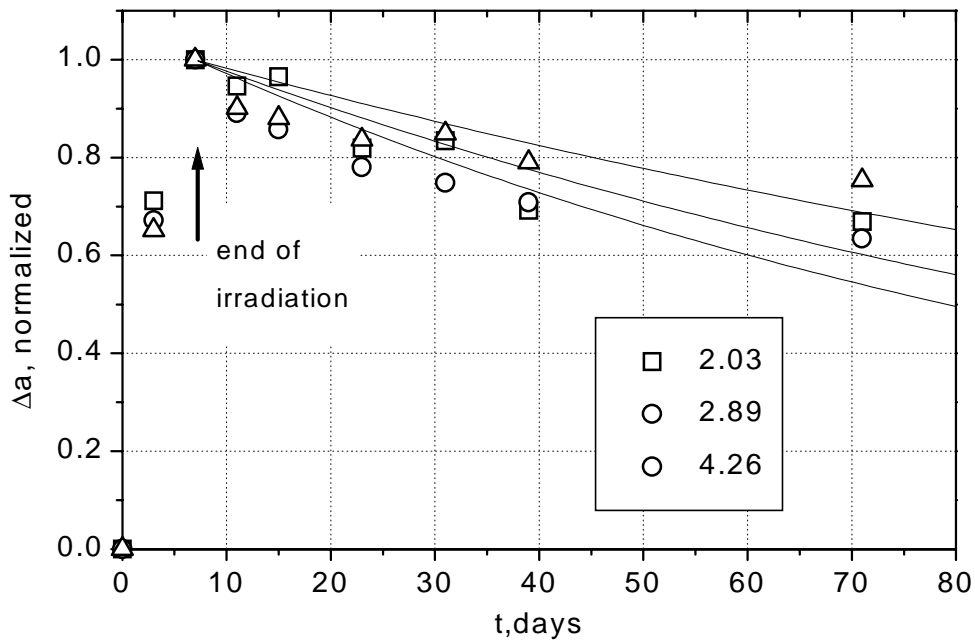


Figure 4 Evolution of the amplitudes of the three visible bands. (Band energies in eV). Solid lines represent fit of the post-radiation relaxation kinetics with exponential decay (Debye) functions.

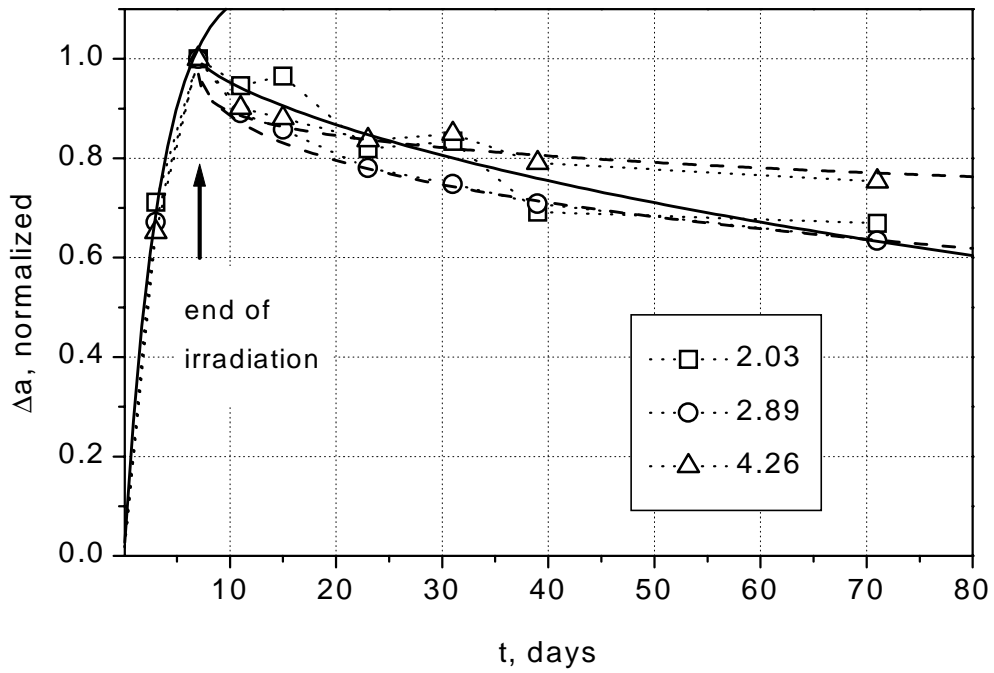


Figure 5 Evolution of the amplitudes of the three visible bands. Solid lines represent fit of the post-radiation relaxation kinetics with stretched-exponential relaxation (Kohlrausch) functions

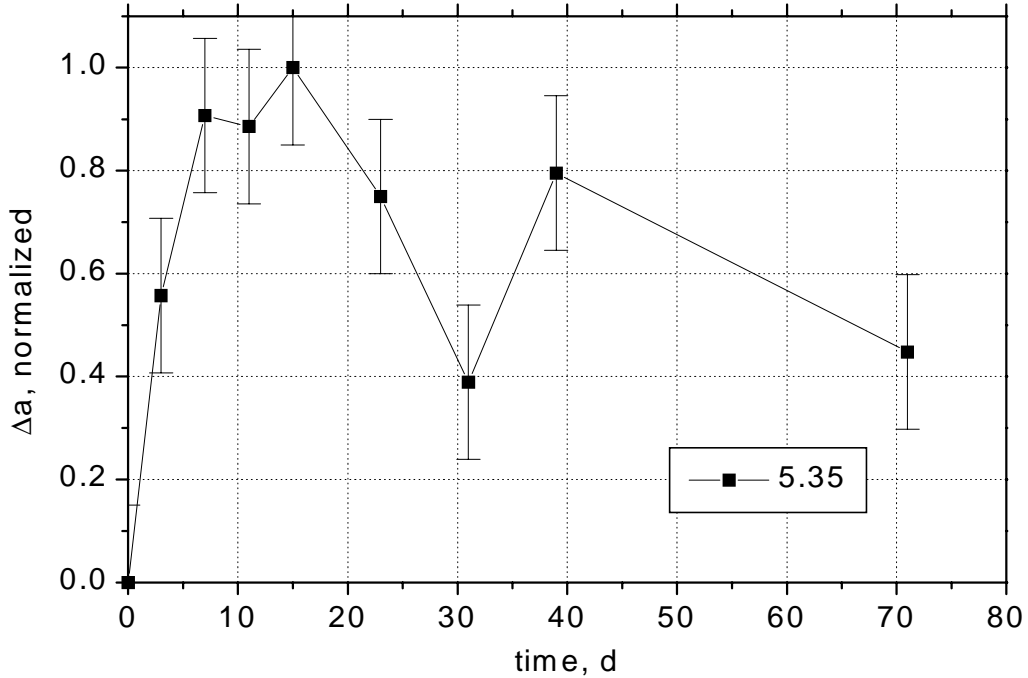


Figure 6 Evolution of the amplitude of the 5.35 eV UV band.

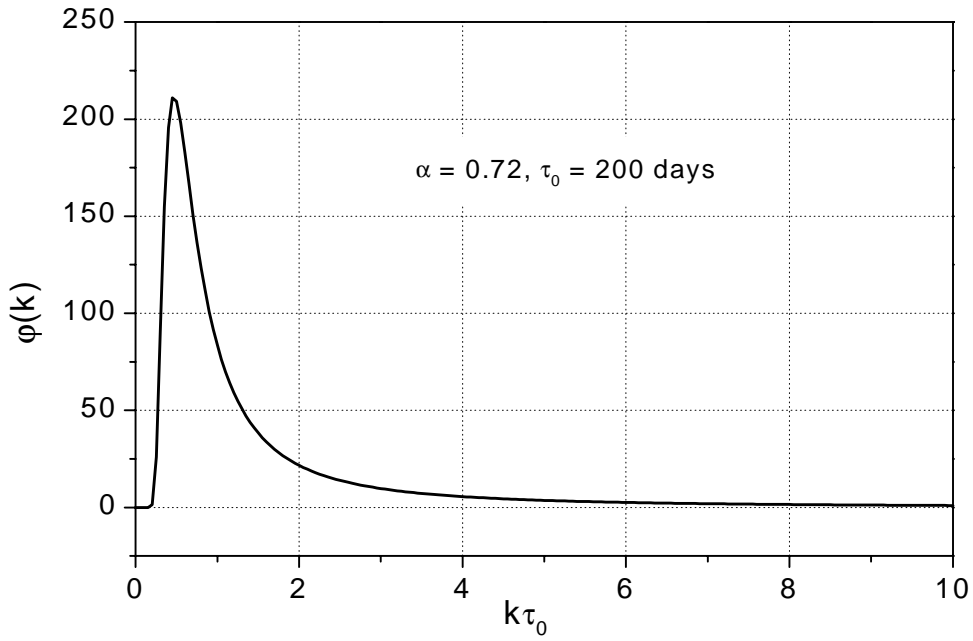


Figure 7 Relaxation rates distribution for a stretched-exponential relaxation function.

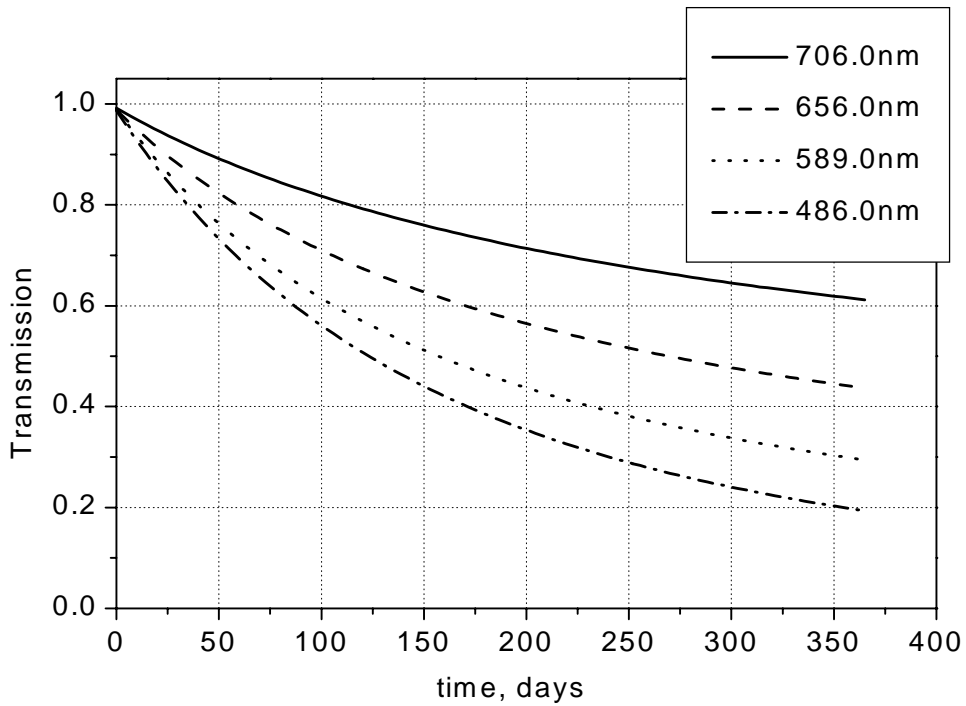


Figure 8. Model simulation of the transmission degradation of a 5-cm thick BK7 glass plate in the course of irradiation up to a total dose of 100 krad over one year. This is typical of a space optical instrument scenario.